

Pseudopotential crystal-structure stability calculations on black phosphorous as a function of pressure

D. Schiferl*

*Department of Geophysics and James Franck Institute, University of Chicago, Chicago, Illinois 60637
and Max-Planck-Institut für Festkörperforschung, 7 Stuttgart 80, Federal Republic of Germany*

(Received 28 February 1978)

The pseudopotential approach is used to make exploratory calculations of the structure-dependent part of the cohesive energy U_s of black phosphorous in a variety of crystal structures as a function of atomic volume. The calculations assume black phosphorous to be a simple sp metal, and empirical local pseudopotentials from the literature were used to fit a modified "empty-core" pseudopotential form. The effects of considering covalent contributions are also considered but not calculated here. At the 1-bar atomic volume, the $A-7$ structure is found to be more stable than the observed black P orthorhombic. However, the difference between U_s (orthorhombic) and $U_s(A-7)$ increases as the atomic volume is decreased, in agreement with the observed transition from the orthorhombic structure to the $A-7$ at 50 kbar. At smaller atomic volumes, the calculations also yield a first-order $A-7$ to simple cubic transition which corresponds to the one observed experimentally at 110 kbar. Although it is possible to imagine a continuous, second-order deformation of the $A-7$ to the simple cubic, the calculations predict discontinuous behavior. The simple cubic is predicted to remain more stable than the fcc, bcc, or hcp structure for a wide range of very high pressures.

I. INTRODUCTION

Black phosphorous, which is the stable form of phosphorous under normal conditions,^{1,2} shows an interesting sequence of structural transformations in the pressure range 0-110 kbar.³ At 1 bar, black P is a narrow-band-gap semiconductor with an orthorhombic crystal structure. The local atomic arrangements suggest that the bonding might be predominantly covalent. At 50 kbar, there is a reversible transformation to a semi-metallic form with the rhombohedral "arsenic" ($A-7$) structure. The local arrangements of atoms are only slightly changed, however. At 110 kbar, there is a second reversible, first-order transition, this time to a *primitive simple cubic (sc) metal*. Again the relative positions of nearest-neighbor atoms change only a small amount during the transformation, but the bonding character is now purely metallic. The simple-cubic form of black P is also interesting because the only other example of an element in a primitive simple-cubic structure is the low-temperature form of polonium.

The pressure-induced orthorhombic to $A-7$ transition was predicted by Parthé from space-filling criteria.⁴ This was one of the first (and is still one of the few!) correct predictions of high-pressure phase transformations. Nonetheless, a more complete understanding of the phase behavior of black P from a more fundamental point of view has not yet been presented. In addition, black P appears to be an ideal material for studying transformations from predominantly covalent bonding

to metallic bonding.

Pseudopotential theory has been used with considerable success in understanding the differences in cohesive energy between competing crystal structures for a variety of sp metals.⁵⁻¹² When all the refinements are used, the theory is quite complex. However, quite reasonable results have been attained using only local pseudopotentials.^{5, 13-17} While such calculations are not always completely successful in predicting the correct crystal structures, they provide valuable insights as to why the observed structures are indeed the stable ones.

Most of the previous structural calculations have been restricted to materials with valence $z \leq 4$. For materials with $z \geq 4$, there are a number of difficulties that arise. Terms higher than second-order are generally expected to yield significant contributions to the cohesive energy, although the author is not aware of any rigorous formulation including all third-order effects. In many cases, a screening function appropriate to semiconductors rather than metals should be used. Special attention should also be given to the Brillouin planes covering the Fermi surface. Moreover, the difficulties in correctly accounting for exchange and correlation contributions are increased for the elements with $z \geq 4$.

In spite of these difficulties, several structure calculations have been done for the high-valence elements. The most recent and most sophisticated is an $X\alpha$ -pseudopotential calculation by Hafner for the pressure-induced phase transitions in tin.¹⁸ Previously, Weaire¹⁵ made local pseudopotential structure calculations for Si in the face-

centered-cubic (fcc), white tin (A-5), and diamond (A-4) structures.

The earliest attempt to understand the arsenic structure and the rhombohedral IV-VI compounds using a pseudopotential approach was made by Cohen, Falicov, and Golin (CFG).¹⁹ The CFG calculations concern the effects of crystal structure changes upon electronic states near the Fermi surface, but those authors did not attempt to calculate the cohesive energy for the different structures. Weaire and Williams¹⁶ (WW) made local pseudopotential calculations for arsenic and antimony, in which they found the rhombohedral arsenic structure to have a lower calculated cohesive energy than the fcc, bcc, hcp, or sc structures. Finally, Abe, Okoshi, and Morita¹⁷ (AOM) have completed local pseudopotential calculations for As very similar to those reported here for black phosphorous.

The present approach is similar to those mentioned above of Weaire for Si and WW and AOM for arsenic. This is a second-order perturbation-theory calculation with local pseudopotentials, which is described in greater detail in Secs. III and IV below. Metallic (Lindhard) screening is used and the Brillouin-zone planes near the Fermi surface are given no special treatment. Thus, the covalent effects implicitly considered in the CFG calculations are ignored here. As the atomic volume is decreased, this procedure becomes more and more justified. However, the principal advantage of this approach is that it allows the calculation of relative cohesive energies for various crystal structures in a simple and straightforward manner. More sophisticated calculations are much more difficult and expensive to perform and are, therefore, not well suited to the type of exploratory calculation reported here. Because the results of these calculations are physically reasonable and

interesting, as shown below, it seems reasonable to do more detailed calculations.

In this paper, the second-order perturbation calculations are applied to black phosphorous. The stability of the observed orthorhombic structure relative to the fcc, bcc, A-4, A-7, and sc structures as a function of volume (i.e., pressure) is considered. In Sec. VII, the reasons that the CFG and the second-order pseudopotential approaches of WW and AOM both predict the A-7 structure to be more stable than the simple cubic are explored by patching up the second-order calculation to include covalent contributions from the Jones zone planes near the Fermi surface in a manner similar to that of Heine and Jones,²⁰ and Weaire¹⁵ for Si. As shown below, inclusion of these covalent contributions should also improve the calculated relative stability of the observed "black P" orthorhombic to the A-7 structure.

II. CRYSTAL STRUCTURES

There are quite a number of crystal structures to be considered in this work. Black P actually attains three different structures in the pressure range 0–110 kbar, and there are several other possible structures that are worthwhile considering. Unfortunately, there is no systematic notation covering all the structures mentioned here. For this reason, common abbreviations are used here, supplemented by the *Strukturbericht*²¹ notation when possible. In a few other cases, quotation marks are used around the name of an elemental form when it is used to refer to a structure type, e.g., "black P" orthorhombic. To avoid confusion, the structures considered here are listed in Table I with their abbreviations in the text. Also listed are key crystallographic parameters, as discussed below, and the packing

TABLE I. Abbreviations used in this work for some crystal structures. Also given are the packing fractions P and descriptions of the structures in terms of the A-7 parameters α and u , where possible.

Structure type	Abbreviation(s)	P	Parameters
face-centered cubic	fcc, A-1	0.740	$\alpha = 60^\circ$ $u = 0.250$
body-centered cubic	bcc, A-2	0.680	$\alpha = 109.47^\circ$ $u = 0.250$
diamond cubic	A-4	0.340	$\alpha = 90^\circ$ $u = 0.125$
"arsenic" rhombohedral	A-7	0.284	$\alpha = 84^\circ$ $u = 0.199$
		0.355	$\alpha = 84.5^\circ$ $u = 0.221$
simple cubic	sc, A-15	0.524	$\alpha = 90^\circ$ $u = 0.250$
face-centered rhombohedral	fcrr
close-packed hexagonal	cph, A-3	0.740	$c/a = \sqrt{8}/3$
"white tin" tetragonal	A-5	0.535	$c/a = 0.5456$
"Bi II" monoclinic	"Bi II"	0.526	$b/a = 0.9165,$ $c/a = 0.4951$
"black P" orthorhombic	"black P"	0.332	$b/a = 2.394,$ $c/a = 0.7572$
			$u = 0.081$ $v = 0.104$

fractions P .

The most important structures in discussing the behavior of black phosphorous are the $A-7$, sc , and "black P" orthorhombic. These structures and their relations to each other and to some other structures are described below.

The $A-7$ structure is rhombohedral¹ with space group $R\bar{3}m (D_{3d}^6)$ and can be considered as two interpenetrating face-centered rhombohedral (fcr) lattices A and B with rhombohedral angle α .¹⁹ The origin of the A sublattice is at $(0, 0, 0)$, while that of the B sublattice is at $(2u, 2u, 2u)$. CFG and WW choose their rhombohedral axes to be from the origin to the midpoints of the face diagonals of the fcr lattice. In that case, the values $\alpha = 60^\circ$ and $u = 0.250$ describe a simple cubic structure. Throughout this paper we shall use the alternative set of rhombohedral axes consisting of the edges of the fcr lattice. For this choice of axes, $\alpha = 90^\circ$ and $u = 0.250$ is sc ; $\alpha = 90^\circ$ and $u = 0.125$ is the $A4$; $\alpha = 60^\circ$ and $u = 0.250$ is fcc , and $\alpha = 109.47^\circ$ and $u = 0.250$ is bcc .

The structure of black P at 1 bar is orthorhombic¹ with space group $Acam (V_{h}^{18})$ and lattice constants $a = 4.3763 \text{ \AA}$, $b = 10.4780 \text{ \AA}$, $c = 3.3136 \text{ \AA}$. There are eight atoms in the unit cell, which are located at

$$\begin{aligned} &\pm (u, v, 0), \quad \pm (u + t, \bar{v}, \frac{1}{2}) \\ &\pm (u, v + \frac{1}{2}, \frac{1}{2}), \quad \pm (u + t, \frac{1}{2} - v, 0), \end{aligned}$$

where $t = \frac{1}{2}$, as explained below, $u = 0.081$, and $v = 0.1017$.

The "black P" structure is closely related to both the simple cubic and $A-7$ rhombohedral structures. Figs. 1(a) and 1(b) show the relation between the "black P" orthorhombic [Fig. 1(a)] and the simple cubic referred to orthorhombic axes [Fig. 1(b)]. The bond angles are changed from 90° in the orthorhombic structure, but the most striking difference between the two structures is the double-layer shift involving the atoms labeled 3, 4, 5, and 6 in both figures. The simple cubic structure is attained when $a = c = b/(2\sqrt{2})$ and $u = 0, v = \frac{1}{8}, t = 0$.

The relation of the bonding arrangements in the black P and $A-7$ structures is shown in Fig. 2. In both cases, the atoms are arranged in double layers. With slight changes (on the order of 1%) in the orthorhombic lattice constants and position parameters, atoms in both structures would have the same first and second nearest neighbors. The third nearest neighbors are different.

As discussed in the introduction, black phosphorous has the orthorhombic structure up to about 50 kbar where it transforms to the $A-7$ structure. The $A-7$ structure is stable in the range 50 kbar

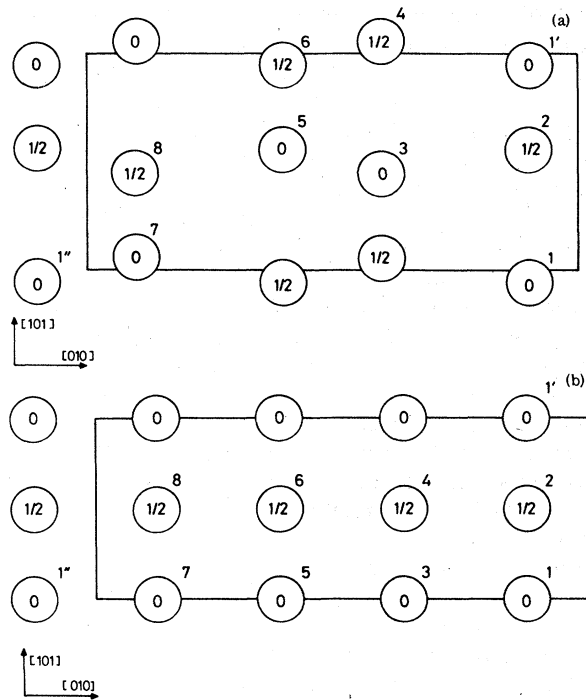


FIG. 1. Relation between "black P" orthorhombic [Fig. 1(a)] and simple cubic referred to the orthorhombic unit cell [Fig. 1(b)]. The vertical cell axis is the a axis and the horizontal one is the b axis. The arrows at the lower left give the orientation of the simple cubic cell relative to the orthorhombic cell. The fractions indicate displacements out of the plane of the drawing in units of the lattice constant c .

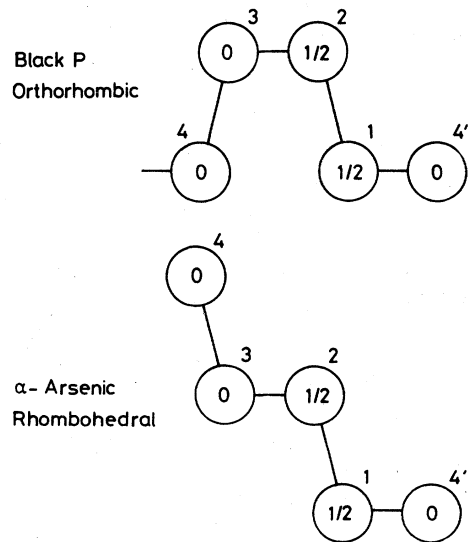


FIG. 2. Relation between bonding arrangements in the "alpha-arsenic" rhombohedral ($A-7$) and "black P" orthorhombic structure. The fractions indicate displacements out of the plane of the drawing in units of the orthorhombic lattice constant c .

to ~110 kbar where it undergoes a *first-order* phase transition to the simple cubic structure.³ This is quite a wonderful transition, first, because it results in a primitive simple cubic cell at all, second, because the transition is *first order*. Geometrically, one can imagine a continuous variation of α and u so that the A-7 structure deforms continuously into the simple cubic,¹⁹ such a continuous process would result in a *second-order* transition.

Finally, the other group-V elements, As, Sb, and Bi, should be mentioned even though no calculations for them are reported here. The experimental situation is somewhat different for each element, and it is useful to have all the structural information of the group-V elements in mind.

The stable structure of As at 1 bar is the A-7,¹ although ϵ -As is metastable with the black P structure. No experimental values of u and v are known for ϵ -As. As pressure is increased for the rhombohedral structure, $\alpha \rightarrow 90^\circ$ and $u \rightarrow 0.250$.²² The A-7 structure is reported to transform to an unknown structure at about 120 kbar.²³

At 1 bar, the stable structure of Sb is also the A-7.¹ As with As, $\alpha \rightarrow 90^\circ$ and $u \rightarrow 0.250$ with increasing pressure.^{24, 25} A first-order transition at 70 kbar to the simple cubic structure is reported by some workers²⁶⁻²⁸ but not found by others.^{29, 30} Other transitions are reported at higher pressures.²⁶

Bi has the A-7 structure at 1 bar, and, under pressure, $\alpha \rightarrow 90^\circ$ and $u \rightarrow 0.250$, just as in As and Sb. However, in contrast to the behavior of black P, Bi transforms to the monoclinic "Bi II" structure,³¹ not the simple cubic.

III. PSEUDOPOTENTIAL STRUCTURE CALCULATIONS

The theory of pseudopotential calculations of crystal structures has been treated extensively by other authors.^{5-7, 32-35} For that reason this section is devoted primarily to the features of special importance to these calculations. With slight departures for clarity, the notation used here is that of Heine and Weaire.⁵ Their convention of using q to denote a continuous variable and g to mean a reciprocal-lattice vector is also followed here.

The cohesive energy per atom of a metal or narrow-gap semiconductor can be divided into a structure-independent part and a structure-dependent part U_s . It is only this latter part that is calculated in this work. For a metal, U_s can be written as the sum of two terms:

$$U_s = U_E + U_{BS}, \quad (3.1)$$

where U_E is the electrostatic (Ewald) energy of

positive ions in a uniform, static electron sea, and U_{BS} is the band-structure energy.

A. Ewald energy

In atomic units,³⁶ U_E is given by

$$U_E = \alpha_E Z^* / 2R_a, \quad (3.2)$$

where R_a is the atomic radius, Z^* is the effective valence, and α_E is the Ewald constant. The method of Sholl³⁷ and Ewald-Fuchs³⁸ method were both used to calculate α_E . A computer program provided by J. Hafner³⁹ was used for the Ewald-Fuchs calculations.

The effective valence Z^* is given by

$$Z^* = Z(1 + \eta), \quad (3.3)$$

where Z is the actual valence ($Z = 5$ for P) and η is the dimensionless orthogonalization hole parameter. There are several ways to determine η .^{5, 32} The method used here was to use the approximate relation

$$\eta \approx (R_c / R_a)^3, \quad (3.4)$$

where $R_c \approx \frac{1}{2} \pi / q_0$ as suggested by the "empty core" model.⁵ The value $R_c = 0.8503851$ a.u. was used for the results reported here, but values in the range $0 < R_c < 1$ a.u. were also tried for a number of trial calculations. Because it always turns out that $\eta \leq 0.1$, fairly large percentage errors in R_c make very little difference in the final structures found to be stable. It should be noted that η comes from the energy dependence of the pseudopotential.

The local pseudopotentials that were finally used in this work are independent of energy, and thus it is slightly inconsistent to use anything other than $R_c = 0$ in Eq. (3.4). However, none of the structural trends are changed by replacing the actual value of R_c used with $R_c = 0$.

B. Band-structure energy

The band-structure energy is given by

$$E_{BS} = \sum_{\vec{g}}' S^*(\vec{g}) S(\vec{g}) F(g), \quad (3.5)$$

with the prime indicating that $g=0$ is omitted from the sum, with $g = |\vec{g}|$, and with $F(g)$ the energy-wave-number characteristic.^{6, 33} Equation (3.5) is perfectly general in that no assumption has to be made as to whether $F(g)$ will be constructed from local or nonlocal pseudopotentials or as to how exchange and correlation corrections will be handled.^{6, 33}

In the case of local pseudopotentials, $F(q)$ takes a particularly simple form

$$F(q) = |V(q)|^2 \chi(q) \epsilon(q), \quad (3.6)$$

where $\chi(q)$ is the Lindhard function and $\epsilon(q)$ is the wave-vector dependent dielectric function,⁵ $V(q)$ is obtained from Eqs. (4.1) and (4.2) below. The Lindhard function $\chi(q)$ is given by

$$\chi(q) = -\frac{1}{2} Z \left(\frac{2}{3} E_F\right)^{-1} \left(\frac{1}{2} + \frac{4k_F^2 - q^2}{8qk_F} \ln \left| \frac{q + 2k_F}{q - 2k_F} \right| \right) \quad (3.7)$$

and $\epsilon(q)$ is given by

$$\epsilon(q) = 1 - (8\pi/\Omega q^2) [1 - f(q)] \chi(q), \quad (3.8)$$

where the factor $[1 - f(q)]$ corrects for correlation and exchange. Three forms for $f(q)$ were considered in the present work. The first is the Hubbard-Sham^{5,40,41} form

$$f(q) = \frac{1}{2} q^2 / (q^2 + k_F^2 + k_s^2), \quad (3.9)$$

where $k_s^2 \approx 2k_F/\pi$.

The second form is due to Shaw.^{5,33}

$$f(q) = \frac{1}{2} [1 - \exp[-\frac{1}{2} (q/k_F)^2 (1 + 0.0254r_s)]]], \quad (3.10)$$

where r_s is the electron density parameter given by

$$r_s = Z^{-1/3} R_a.$$

Finally, the third form is simply no correction at all,

$$f(q) = 0 \quad (3.11)$$

The Hubbard-Sham form, Eq. (3.9), and the Shaw form, Eq. (3.10), yielded very close to the same $A-7$ structures of minimum energy at all atomic volumes tested. Somewhat different values of u and α were obtained with $f(q) = 0$, and the agreement with the observed structure at 1 bar was worse. The calculations reported here were all done assuming the Shaw form, Eq. (3.10), unless otherwise indicated.

IV. PSEUDOPOTENTIALS

In these calculations, local pseudopotentials were used throughout. Nonlocal pseudopotential calculations are better justified, but are much more difficult and expensive to perform.^{5,18}

When local pseudopotentials are used, the total Fourier component $V(g)$ can be written as the product

$$V(g) = S(g)v(g), \quad (4.1)$$

where $S(g)$ is the structure factor, $v(g)$ is the pseudopotential form factor, and \vec{g} is a reciprocal-lattice vector with modulus $g = |\vec{g}|$.

The pseudopotentials used here were derived from the empirical pseudopotentials compiled by Cohen and Heine.³² An interpolation function was fitted to this data so that a consistent set of $v(g)$'s

could be generated for the changing values of the g 's under pressure. Because the orthorhombic "black P" structure has some very small g 's beyond the range of the experimentally determined $v(g)$, it is necessary to choose an interpolation function $v(q)$ which has the correct limiting value $v(q \rightarrow 0) = -\frac{2}{3} E_F$ and has some theoretical justification as well. The Lin and Falicov form,^{42,43} which was used to fit the Fermi-surface data in the first place, is inadequate for this purpose as it is unreliable at small q . The "empty core" model of Ashcroft⁴⁴ satisfies these criteria but cannot be used to fit the empirical $v(g)$ very well. A "modified empty core" model was chosen of the form

$$V(q) = [-4\pi Z / q^2 \epsilon(q) \Omega] \cos(q\pi/2q_0) C(q) D(q) \quad (4.2)$$

with

$$C(q) = A_1 / (A_1 + q^n), \quad (4.2a)$$

and

$$D(q) = [1 + \exp[A_3(-A_4)]] / [1 + \exp[A_3(q^2 - A_4)]] \quad (4.2b)$$

In Eq. (4.2), Z is the valence, $\epsilon(q)$ is the dielectric response function, Ω is the atomic volume, and q_0 is the position of the first zero of $v(q)$. In Eqs. (4.2a) and (4.2b), A_1 , A_3 , A_4 and n are fitting constants.

The factor $C(q)$ modifies the curvature of $v(q)$ to fit the literature values in the range $0.5 \lesssim q \lesssim 1.0$ a.u. The value $n=2$ was used in the calculations reported here; however, $v(q)$ could have been fitted with $n=1$ or $n=3$ (and different values of A_1 , A_3 , and A_4). The relative stability of the different structures did not depend strongly on n .

The factor $D(q)$ in Eq. (4.2) damps $v(q)$ so that for $q \geq 1.5$ a.u. $v(q) \approx 0$ in accordance with the empirical values. Both $C(q)$ and $D(q)$ tend to unity as $q \rightarrow 0$. Thus, $v(q)$ is essentially the pure "empty core" form at very small q . At each pressure, the renormalization for the changed atomic volume Ω , and dielectric response $\epsilon(q)$ is correctly included through the "empty core" part of Eq. (4.2).

The empirical $v(q)$ came from semiconductor data collected by Cohen and Heine.³² Equation (4.2) for $v(q)$ of phosphorous was fitted to this combined data after appropriate renormalization for the change in Ω and $\epsilon(q)$ in going from a compound (such as InP) to the pure group-V element (such as P).

The resulting $v(q)$ were fitted with appropriate values of q_0 , n , A_1 , A_3 , and A_4 ; these quantities were then varied within the limits of the experimental uncertainty of the $v(q)$ values for the best fit to the observed 1-bar crystal structures. Within these limits the relative stability of different structures was rather insensitive to the choices of

TABLE II. Pseudopotential parameters used in Eq. (4.2).

$q_0 = 1.693\ 350\ 4$ a.u.
$n = 2$
$A_1 = 7.000\ 575\ 1$ a.u.
$A_3 = 2.834\ 617\ 1$ a.u.
$A_4 = 4.004\ 329\ 0$ a.u.

q_0 , n , A_1 , A_3 , and A_4 . The values of these quantities and R_c are given in Table II; and the resultant $v(q)$ curve, along with the empirical values from Cohen and Heine,³² is shown in Fig. 3.

Finally, to keep the number of parameters varied to a minimum, q_0 was kept constant. This is equivalent to assuming that the radius R_c of the ion core is constant.³²

V. CALCULATION PROCEDURE

The calculations are nominally performed at 0°K; entropy is not considered. Actually, cohesive energies of the 1-bar structures were calculated using the room-temperature atomic volumes. Low-temperature lattice constants are not available for black P. In α -As, Sb, and Bi the differences between the low-temperature and room-temperature values of α and u are very small experimentally⁴⁵⁻⁴⁷ and are considerably smaller

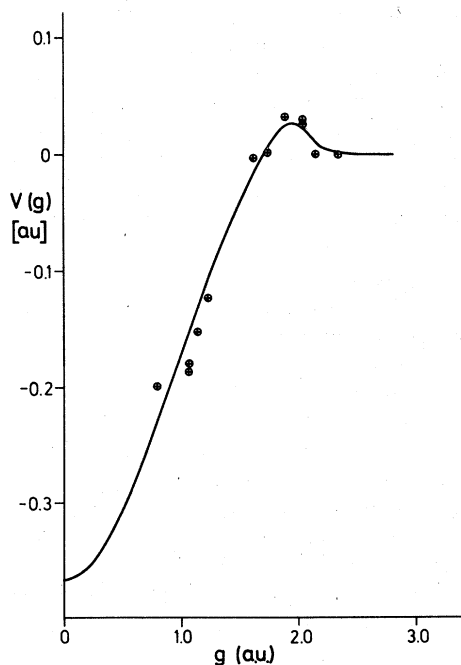


FIG. 3. Phosphorous pseudopotential form factor $V(g)$. The circles represent empirical pseudopotential values from Ref. 32. The line is calculated according to Eq. (4.2) with the values of Table II.

than the errors in these calculations.

In considering the relative stability of different crystal structures, care was taken to keep the atomic volumes constant to within 1 part in 10^7 .

In the "black P" orthorhombic structure, there are six variables a , b , c , u , v , and t . This is too many parameters to vary together in any meaningful way. The only values of a , b , and c used were the observed values, or the values $a = c = b/(2\sqrt{2})$ which correspond to the simple cubic referred to the axes of the orthorhombic cell. For both sets of lattice constants, u , v , and t were varied to find the values at which U_s was a minimum. A similar problem is encountered with the "Bi II" monoclinic structure; in that case the observed structure in Bi was scaled down to yield the correct Ω_0 for black P.

The pressure dependence of α and u for the A-7 structure was investigated by reducing the volume per atom Ω . Calculations of U_s were then performed for the values of α and u in the ranges $60^\circ \leq \alpha \leq 94^\circ$ and $0.125 \leq u \leq 0.250$, respectively.

The calculations were performed with double-precision arithmetic on an IBM 370/168 computer at the University of Chicago Computation Center, or on a Honeywell-Bull computer at the Max-Planck-Institut für Festkörperforschung, Stuttgart.

VI. RESULTS

A. One-bar structures

The values of U_s for several possible structures for black P are given in Table III. In the orthorhombic structure, the calculations were done using the observed lattice constants, but allowing the atom positions u and v to vary. Table III contains values of U_s for the observed values ($u = 0.081$ and $v = 0.1017$), as well as those which yielded the minimum U_s ($u = 0.081$ and $v = 0.106$). In view of the total success of all the calculations reported here, the very close agreement between the two sets of parameters must be regarded as somewhat fortuitous.

As can be seen from Table III, the orthorhombic structure was also calculated to have a lower energy than the sc, bcc, or fcc; however, the A-4 and the A-7 both had even lower values of U_s . Of the A-7 structures considered, the most stable was found to be an A-7 with $\alpha = 84^\circ$ and $u = 0.199$. At 1 bar, the A-7 structure is not even metastable, so these results cannot be directly compared with experiment. However, Jamieson³ finds the high-pressure A-7 form to have $\alpha = 87.6^\circ$ and $0.21 \leq u \leq 0.22$. In view of the fact that α and u both tend to increase with pressure in As and Sb,^{22, 24, 25} the calculated 1-bar A-7 cannot be regarded as a particularly disheartening result.

TABLE III. Structure-dependent part U_s of the cohesive energy for the "black P" orthorhombic structure with $\Omega = \Omega_0$. U_s is also given for the A-4 and most stable A-7 structures.

u	v	t	$E(\text{a.u.})$	Comments ^a
0	$\frac{1}{8}$	0	-7.884 19	Simple cubic*
0	$\frac{1}{8}$	$\frac{1}{4}$	-7.863 25	*
0	$\frac{1}{8}$	$\frac{1}{2}$	-7.865 55	*
0	0.160	0	-7.883 69	*
0	0.160	$\frac{1}{4}$	-7.866 97	*
0	0.160	$\frac{1}{2}$	-7.889 01	*
0.080	0.160	0	-7.891 06	*
0.080	0.160	$\frac{1}{4}$	-7.881 39	*
0.080	0.160	$\frac{1}{2}$	-7.898 45	*
0.081	0.1017	$\frac{1}{2}$	-7.900 02	Observed "black P" orthorhombic
0.081	0.106	$\frac{1}{2}$	-7.900 43	Most stable "black P" orthorhombic
$\alpha = 84^\circ$	$u = 0.199$		-7.923 00	Most stable A-7
$\alpha = 90^\circ$	$u = 0.125$		-7.925 32	A-4

^a Asterisk (*) indicates that the lattice constants have the simple cubic ratios of $a = c = b / (2\sqrt{2})$.

B. High-pressure structures

The values of U_s for different values of the rhombohedral angle α and u for the A-7 structure at different Ω are presented as energy "contour maps" in Figs. 4(a)–4(f). At 1 bar, the most stable structure is with $\alpha = 84.0^\circ$ and $u = 0.199$ as discussed above. As Ω is decreased from the 1-bar value of Ω_0 , u increases reasonably rapidly while α increases very slowly. The trends are qualitatively correct for both u and α . No experimental data is available for the variation of either u or α in black P; however, these same qualitative trends are seen in u and α in As, Sb, and Bi under pressure.^{22–31}

The most interesting feature of these calculations begins to appear when $\Omega = 0.91 \Omega_0$ [Fig. 4(c)]. At that atomic volume, a second local minimum first appears for the simple cubic structure ($\alpha = 90^\circ$, $u = 0.250$). When α is decreased just a small amount more to $\Omega = 0.892 \Omega_0$, the "simple cubic" minimum and the "rhombohedral minimum" at $\alpha = 84.5^\circ$ and $u = 0.220$ have nearly identical values of U_s [Fig. 4(d)]. By the time $\Omega = 0.885 \Omega_0$ [Fig. 4(e)], the "rhombohedral minimum" simply disappears without the values of α and u having changed substantially; only the minimum around the simple cubic remains. *In other words, the*

calculations predict quite unambiguously that the A-7 to simple cubic transition in black P should be a first-order transition. This is observed to be the case, as mentioned above in Sec. II. Further compression to $\Omega = 0.857 \Omega_0$ and beyond, does not change the situation [Fig. 4(f)].

The values of U_s for a number of structures relative to the simple cubic as a function of Ω are shown in Fig. 5. It is interesting to note that while the observed orthorhombic structure was incorrectly calculated to have a higher energy than the A-7 at 1 bar, it is correctly calculated as increasing relative to the A-7 with decreasing volume. That is, the orthorhombic becomes less stable than the A-7 with pressure, in agreement with experimental trends. It is also interesting to note that the sc structure is calculated to remain stable with respect to the more closely packed bcc, fcc, and hcp structures over an incredibly large range of atomic volumes. Ultimately, U_B will dominate over U_{BS} and the close-packed structures will be preferred over the sc, but this will apparently happen only at far higher densities than treated here.

The way in which some of these trends come about can be seen by looking at the distribution of structural weights $W(g) = \sum |S(g)|^2$ relative to the energy-wave number characteristic $F(q)$. This is shown for $R = R_0$ and $R = 0.96 R_0$ in Figs. 6(a) and 6(b), respectively. At 1 bar ($R = R_0$), both the A-4 and the sc have the greatest $W(g)$ very near q_0 . The fcc and bcc avoid q_0 somewhat, but not as well as the A-7 and "black P" orthorhombic do. In fact, both of these latter structures appear to have very favorable structural weight distributions.

When the volume is reduced so that $R = 0.96 R_0$, the situation changes so as to favor the sc and A-4 over the other structures. The fcc and bcc now have large structural weights around q_0 and, in fact, their situation will worsen for a while as R is further decreased. It is for this reason that the sc is calculated to remain stable over a wide range of high pressures.

While pseudopotential theory seems to be most reliable when small deviations from a given structure are considered, the strongly decreasing stability of the bcc, fcc, and hcp relative to the sc when Ω is decreased suggests that no refinements to these calculations will change this behavior and that this predicted behavior should be taken seriously. High-pressure x-ray diffraction experiments are in progress to check this prediction.

C. Stability of the simple cubic structure at high pressures

It is instructive to examine the balance between the band-structure energy U_{BS} and the electro-

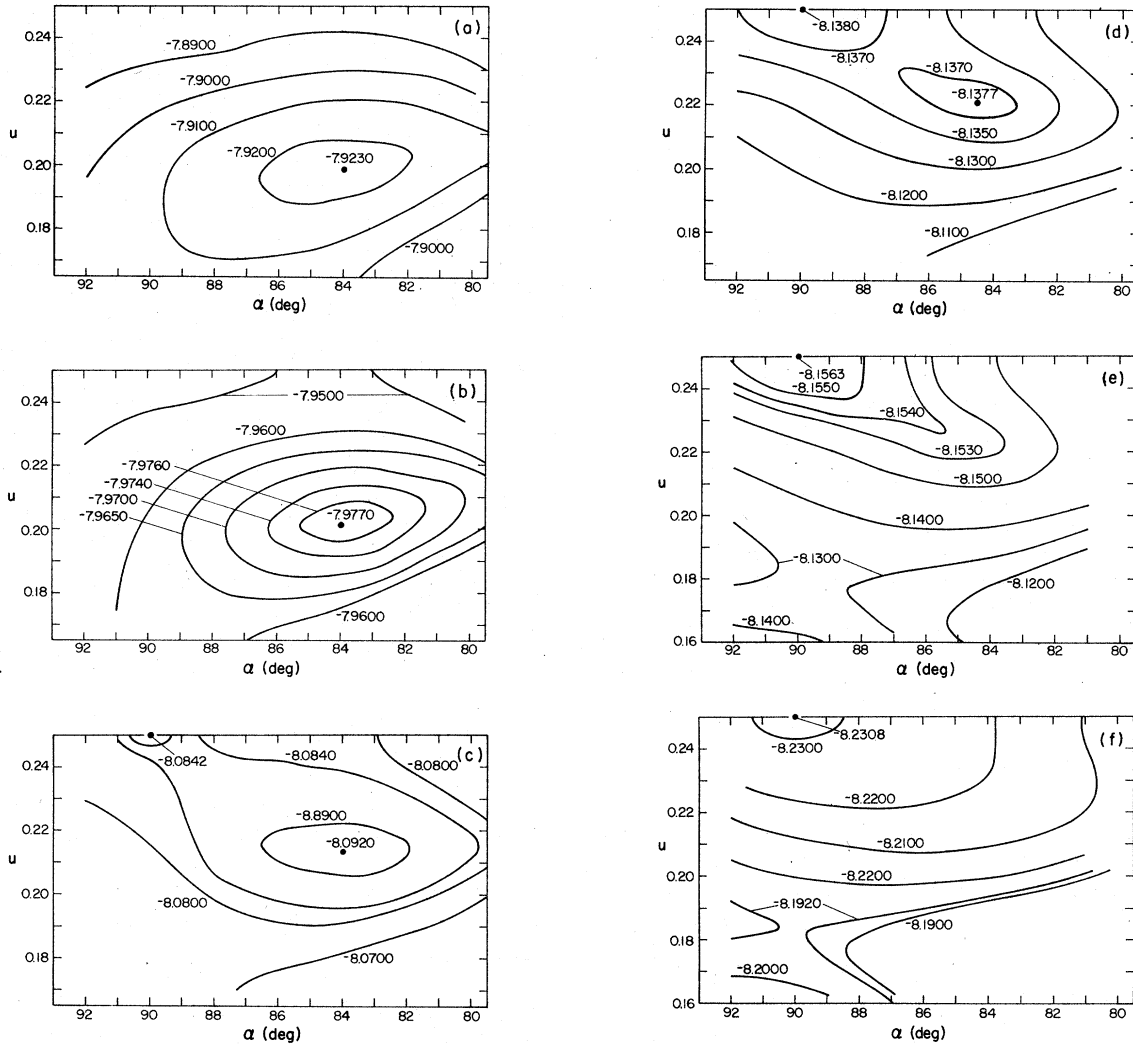


FIG. 4. Structure-dependent part U_s of the cohesive energy for the $A-7$ structure vs α and u for several different atomic radii R_a (i.e., different pressures). (a) $R_a = R_a$ (1 bar), $\Omega = \Omega_0$; (b) $R_a = 0.99 R_a$ (1 bar), $\Omega = 0.9703 \Omega_0$; (c) $R_a = 0.97 R_a$ (1 bar), $\Omega = 0.9127 \Omega_0$; (d) $R_a = 0.9625 R_a$ (1 bar), $\Omega = 0.8917 \Omega_0$; (e) $R_a = 0.96 R_a$ (1 bar), $\Omega = 0.8847 \Omega_0$; (f) $R_a = 0.95 R_a$ (1 bar), $\Omega = 0.8574 \Omega_0$.

static energy U_E that gives rise to the calculated structural behavior. The variation U_E with α and u is shown in Fig. 7. Note that $U_E(\alpha, u)$ is symmetric around $u = 0.250$ and that for fixed α , U_E has a minimum at $u = 0.250$. A less obvious feature also shown in Fig. 6 is that for u fixed at $u = 0.250$, U_E has a weak maximum at $\alpha = 90^\circ$. Thus, $U_E(\alpha, u)$ has a saddle point at $\alpha = 90^\circ$ and $u = 0.250$.

Except for a scale factor to be applied to $U_E(\alpha, u)$, Fig. 7 is invariant with pressure, as can be seen from Eq. (3.2). The ratios of the U_E values for different α and u remain constant because they depend only on the values of the Ewald constants $\alpha_E(\alpha, u)$, which are independent of the atom-

ic volume.

On the other hand, the band-structure energies $U_{BS}(\alpha, u)$ change with pressure in different ways for different values of α and u . Because of this, the exact balance between U_{BS} and U_E , which determines the structure, changes with pressure. This change in the relative strengths of U_{BS} for different α and u is rather subtle, and the general structural trends promoted by U_{BS} remains unchanged over the entire range of atomic volumes considered in these calculations. These trends are generally the opposite of those promoted by U_E . For $u = 0.250$, U_{BS} favors the simple cubic structure with $\alpha = 90^\circ$; however, U_{BS} also strongly

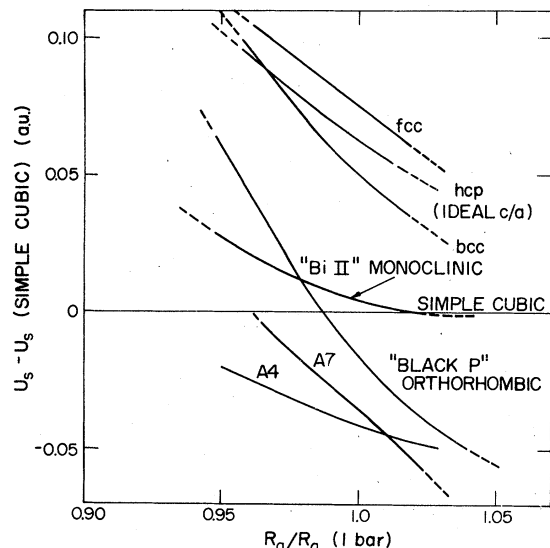


FIG. 5. Relative structure-dependent energies for a variety of crystal structure types as a function of atomic radius $R_a = gR_a$ (1 bar). For each value of g the difference $[U_s$ (structure considered) $- U_s$ (sc)] is plotted.

favors a distortion such that $u \neq 0.250$ and $\alpha < 90^\circ$.

When the atomic volume is small enough, the simple cubic structure is stabilized against a shift of the atom position parameter away from $u = 0.250$ by the electrostatic energy. This is shown in Fig. 8(a), where U_E and U_{BS} are plotted vs u , with $\alpha = 90^\circ$ and $R_a = 0.96 R_a$ (1 bar). It can be seen that U_E has the greater variation with u at this atomic volume. However, the electrostatic energy promotes a shear distortion which would eventually cause the structure to become fcc ($\alpha = 60^\circ$) or bcc ($\alpha = 109.471^\circ$). It is the band-structure energy which stabilizes the structure against this shear distortion. This is shown in Fig. 8(b), where U_E and U_{BS} are shown as functions of α with $u = 0.250$ and $R_a = 0.96 R_a$ (1 bar). In this case, U_{BS} has the greater variation with α .

These observations do not conflict with the conclusion of Born and Huang⁴⁸ that the simple cubic structure is unstable for atoms bound together by pairwise central forces. The total structure-dependent energy U_s can be shown to be of the form of pairwise central forces, but it is not the total potential. In contrast to the case considered by Born and Huang, U_s is only a rearrangement potential at constant volume, and this volume is largely determined by the volume-dependent, but structure-independent total energy contributions, such as the electronic kinetic and correlation energies.⁵

It is by no means certain that these calculations, if repeated for the other group-V elements, As, Sb, and Bi, would yield the simple cubic structure as a form necessarily more stable than the A-7 or "Bi II" monoclinic structures for any pressure.

The changes in U_{BS} with pressure that are required to stabilize the simple cubic may be attained only in black P. Such a variation in the pressure behavior of U_{BS} as we go from black P to As, Sb, and finally, Bi may account for the observed variety of high-pressure structures in the last three of these elements. It may also explain the fact that the simple-cubic structure has never been observed in As or Bi.

If the volume dependence of the balance between U_E and U_{BS} is calculated to be different in As, Sb, and Bi, we might expect such a difference to arise in part from the fact that the 1-bar atomic volumes and q_0 values are different and that nonlocality is important in Bi. Even fairly large changes in the $v(q)$ curves of Fig. 3 do not change the qualitative results of calculations in black P.

VII. COVALENT EFFECTS

In these calculations, black P has been considered as a metal. While this is true if black P takes the fcc, bcc, hcp or sc structures, the A-7 form is probably a semimetal with the Fermi surface almost completely contained in the fifth Brillouin zone, and the orthorhombic form is a small band-gap semiconductor.

In the case of covalent structures, the theory outlined in Sec. III falls apart in several places simultaneously. The critical difference between metallic and covalent (including semimetallic) structures is the separation of filled and unfilled states by a band gap E_g in the covalent structures. This feature gives rise to several important considerations:

A. Dielectric functions

The dielectric response functions $\chi(q)$ and $\epsilon(q)$ from the forms given, respectively, in Eqs. (3.7) and (3.8) are changed to forms depending on the energy gap E_g . The Penn model is the most familiar approximation for this case.^{49, 50} As $E_g \rightarrow 0$, the Penn model forms of $\chi(q)$ and $\epsilon(q)$ approach Eqs. (3.7) and (3.8), respectively. Thus, for nonzero q , use of the metallic forms of $\chi(q)$ and $\epsilon(q)$ is reasonable for small gap semiconductors.

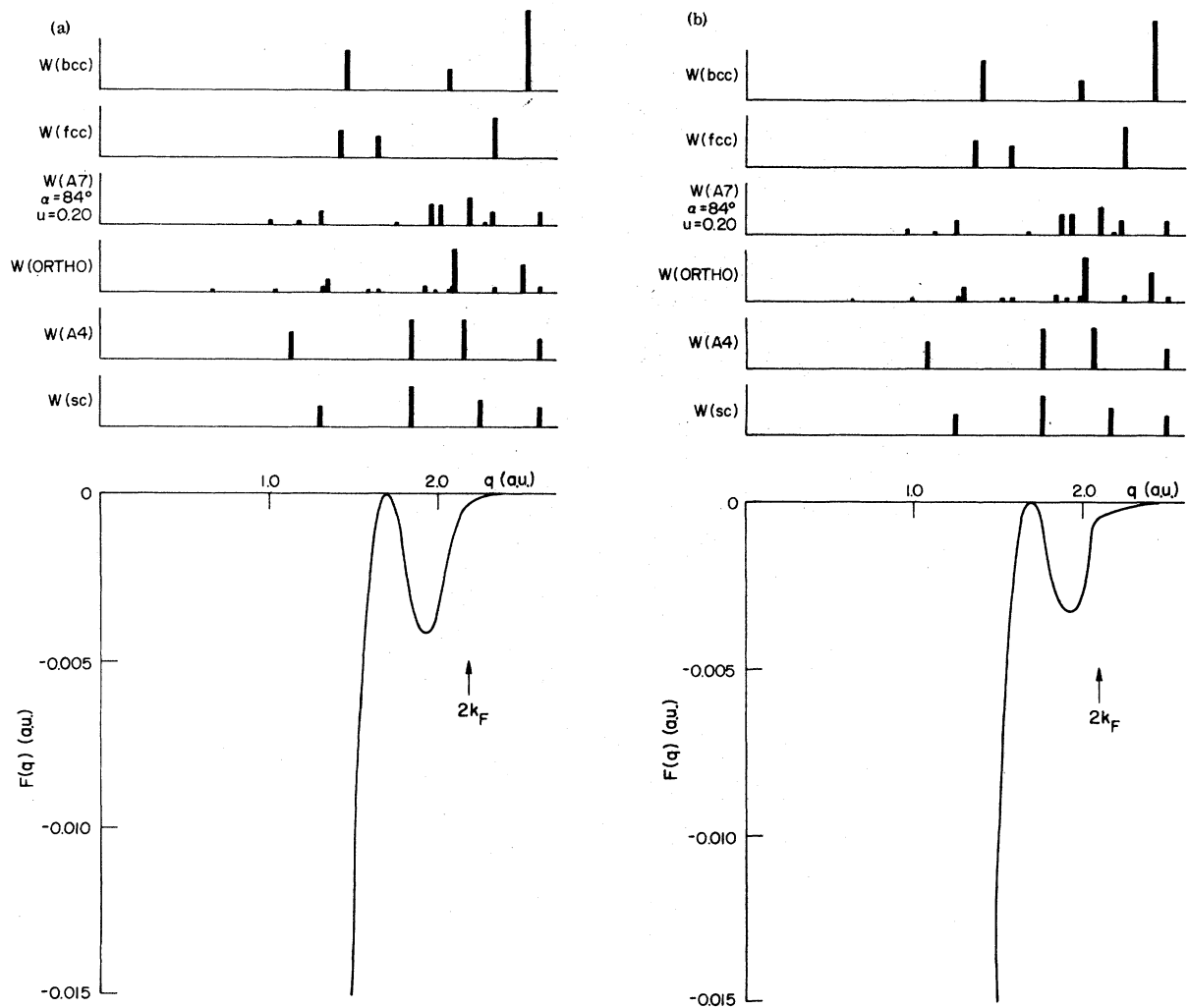


FIG. 6. Structural weights for various structures and the wave-number energy characteristic $F(q)$. (a) $R_a = R_a$ (1 bar) ($\Omega = \Omega_0$). (b) $R_a = 0.960 R_a$ (1 bar) ($\Omega = 0.8847 \Omega_0$).

B. Extra cohesive energy contribution from Jones-zone planes

It is no longer sufficient to consider only isolated Brillouin zone planes as was done in the derivation of Eq. (3.5). There is an extra amount of cohesive energy U_{JZ} per atom resulting from overlap of the Fermi sphere by multiple Jones zone planes. For an isotropic semiconductor, Van Vechten⁵¹ has shown that this is given by the Penn model as

$$U_{JZ} = (3ZE_g^2/16E_F)[1 + \ln(E_g/8E_F)] - \frac{1}{16}(E_g^3/E_F^2)Z. \quad (7.1)$$

When we are faced with real Jones zone planes about the best we can do is estimate an average

gap E_g from the calculated gaps on the centers of the Jones zone faces and apply Eq. (7.1).^{15, 52} This yields only a very approximate estimate of the cohesive energy contribution from the Jones zone planes of course.

C. Higher-order contributions to the Jones zone gap

The gaps of the Jones zone planes are not simply given by $E_g = 2[V(\text{Jones zone})]$, but rather higher-order contributions dominate the gap. Let \vec{g} be the reciprocal-lattice vector spanning opposite sides of Jones zone. If there are reciprocal-lattice vectors \vec{g}_i and \vec{g}_j such that $\vec{g} = \vec{g}_i + \vec{g}_j$ and $V(g_i)$ and $V(g_j)$ are large enough to contribute in second order as much as $V(g)$ in first order, then the Jones zone gap takes the form

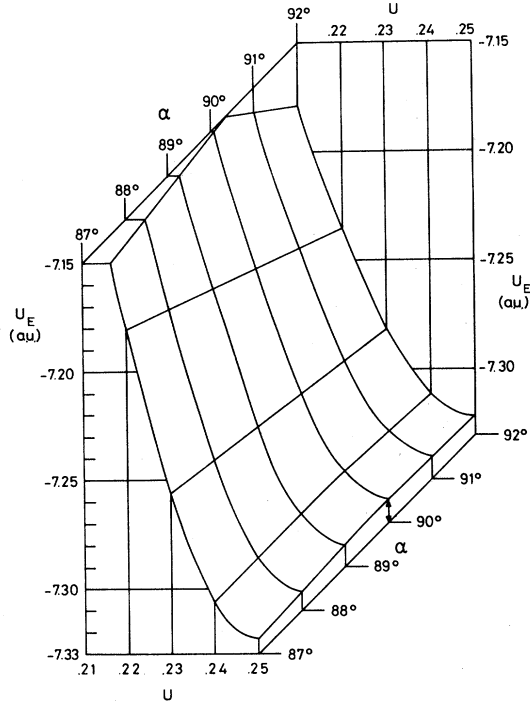


FIG. 7. Variation of the electrostatic (Ewald) energy $U_E(\alpha, u)$. The values of $U_E(\alpha, u)$ are calculated assuming $\Omega = \Omega_0$.

$$E_g = 2 [V_{\text{eff}}(g)] \\ = 2 \left(V(g) + \sum_{\vec{g}_i} \frac{V(\vec{g}_i) V(\vec{g} - \vec{g}_i)}{0.5 \left[\frac{1}{4} g^2 - \left(\frac{1}{2} \vec{g} - \vec{g}_i \right)^2 \right]} \right) \quad (7.2)$$

It has been shown that in IV-VI compounds with the NaCl structure, as well as in the A-7 structure, that the Jones zones are dominated by the $\{131\}$ planes.^{53, 54} Thus,

$$V_{\text{eff}}(311) = V(311) + 4(a/2\pi)^2 \\ \times [V(111)V(200) + V(1\bar{1}1)V(220)] \quad (7.3)$$

for phosphorous in the A-7 structure.

In the simple cubic, referring to the cell described in Sec. II, the structure factors $S(111)$ and $S(311)$ are both zero and the covalent band gap $E_g = 0$. If the atom position u shifts to a value $0.125 \leq u \leq 0.250$, then $S(111)$, $S(200)$, $S(220)$ and $S(311)$ are all nonzero and the Jones zone gap E_g contributes to the cohesive energy in the manner of Eq. (7.1). As has been pointed out before,⁵⁴ this is an additional reason that the other group-V elements, As, Sb, and Bi, take neither the simple cubic nor diamond structures, but rather take the A-7 structure, which is somewhere in between.

D. Higher-order contributions to the Jones zone gap in the black P orthorhombic

Because the orthorhombic structure has a much lower symmetry, the situation is more complicated in this form of black P. Moreover, there are important changes in the identity of the Jones zone planes on going from the A-7 or simple cubic to the orthorhombic. One example illustrates this very well. If the simple cubic cell is referred to the orthorhombic axes, then the (131) and $(13\bar{1})$ planes are written as (160) and (061) , respectively. For the simple cubic structure, all these Jones-zone structure factors are still zero, of course. However, the double-layer shift illustrated in Fig. 1 results in $S(160) \neq 0$, although $S(061) = 0$ still. Changes in the atom position parameters u and v to their values in the observed orthorhombic structure do not change this situation. If the lattice constants maintained their simple cubic ratios $a = c = b/2\sqrt{2}$, black P would be a metal and not a semiconductor. However, the double-layer shift also causes other structure factors to be nonzero, notably, $S(151) \neq 0$. As long as the lattice constants have their simple cubic ratios, the (151) plane does not lie near enough to the Fermi surface. However, the lattice constants of the actual orthorhombic structure are such that the (151) plane lies on the Fermi surface and is thus a Jones zone plane.

The higher-order contributions to $V_{\text{eff}}(151)$ are given by

$$V_{\text{eff}}(151) \\ = V(151) + 2 \left(\frac{V(040)V(111)}{2b^{*2}} + \frac{V(131)V(020)}{3b^{*2}} \right), \quad (7.4)$$

where b^* is a reciprocal lattice constant.

A calculation of $V_{\text{eff}}(151)$ from Eq. (7.4) and $V_{\text{eff}}(131)$ from Eq. (7.3), shows that $[V_{\text{eff}}(151) \approx 2[V_{\text{eff}}(131)]]$. This suggests that when the Jones zone contributions are included for both the A-7 and orthorhombic structures, the orthorhombic structure may well have the lower energy.

This argument is only tentative, of course. Particular Jones zone planes were singled out for this example with no attempt to determine the effects of the others. Moreover, if we are to include the effects of U_{JZ} we should use the covalent forms of $\epsilon(q)$ and $\chi(q)$ of Srinivasan⁵⁰ as well. These calculations are in progress. The results obtained so far are very similar to the second-order calculations presented here, but in better agreement with observed structural trends.

VIII. DISCUSSION

The calculated energy differences between the various 1-bar structures, shown in Table III and

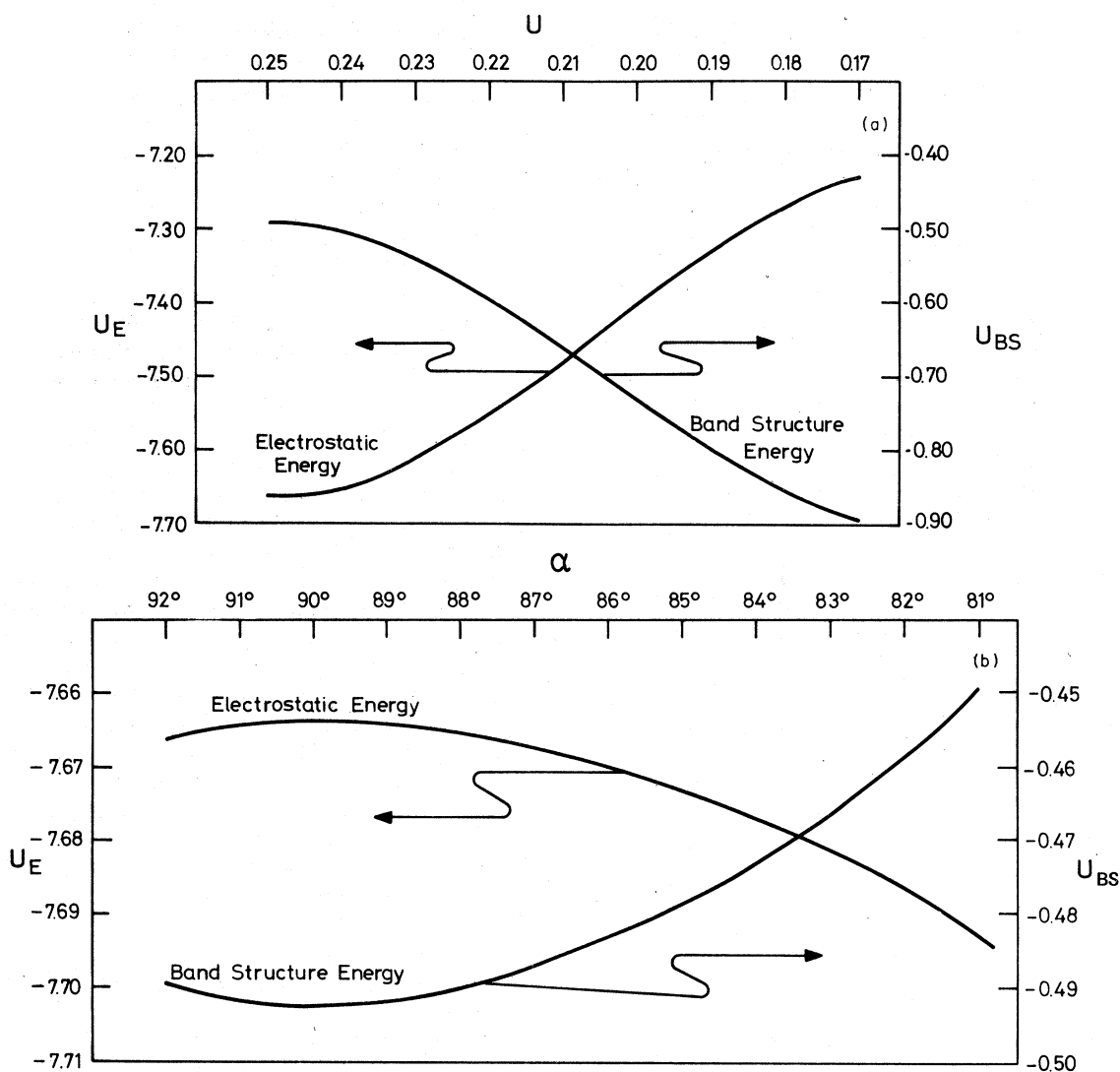


FIG. 8. Variation of $U_E(\alpha, u)$ and $U_{BS}(\alpha, u)$ for $R_a = 0.96 R_a$ (1 bar). In (a), U_E and U_{BS} are plotted vs u with $\alpha = 90^\circ$. In (b), U_E and U_{BS} are plotted vs α with $u = 0.25$.

Fig. 5 are considerably larger than those calculated for lower-valence elements. In view of the fact that second-order local-pseudopotential calculations tend to overestimate distortions, this is a matter of some concern. It turns out that these differences are probably a bit too large, but not unreasonably so.

The only relevant experimental information we have concerning the relative cohesive energies of different structures of phosphorous is the values of the heat of formation H_f^0 for the different allotropes. These are at 25°C and 1 bar⁵⁵ (i) white phosphorous, $H_f^0 = 0.0$; (ii) red phosphorous, $H_f^0 = -4.4$ kcal/mole; (iii) black phosphorous, $H_f^0 = -10.3$ kcal/mole.

The local bonding arrangements in red phos-

phorous and black phosphorous are quite similar and so it is reasonable to expect energy differences between structures to be on the order of 6 kcal/mole ≈ 0.01 a.u./atom. From Table II we see that the differences between the closely related A-7, orthorhombic, and simple cubic structures are calculated to be on the order of 0.01 to 0.04 a.u. This is a bit large but not unreasonable, especially in view of the fact that at $\Omega = \Omega_0$ the orthorhombic structure is calculated to be less stable than the A-7, contrary to experiment.

The general qualitative structural trends described in Sec. VI are quite insensitive to variations in the pseudopotential. Quantitative agreement can be improved with appropriate changes in $v(g)$. For example, it might be argued that the

$v(q)$ values for $q < 1.3$ a.u. might be stronger. As can be seen in Fig. 3, this would improve agreement with several empirical values of $v(q)$, while increasing disagreement with another. Such a change would also improve the stability of the orthorhombic relative to the A-7 at 1 bar and shift all the phase transitions to smaller atomic volumes, in closer agreement with experiment. Such refinements lie outside the scope of this work, which is to see if the general features of the black P phase diagram can be understood in terms of pseudopotential theory in a straightforward manner. They can, and indeed it is remarkable that the second-order pseudopotential approach works so well in describing the structural changes as black phosphorous goes from a semiconductor to a semimetal and finally to a metal.

Some other difficulties in the calculations also remain. As can be seen from Fig. 5, the volume at which the A-7-sc transition takes place is seriously overestimated. In addition, the diamond structure is calculated to be more stable than the simple cubic or A-7 in the range $0.75 \Omega_0 \leq \Omega \leq 1.06 \Omega_0$. It may be hoped that the inclusion of covalent effects through the special treatment of the Jones zone planes, as discussed in Sec. VII above, will correct this problem, at least for the A-7. In black P, or any pentavalent element for that matter, there are no Jones zone contributions for the A-4 or sc. This is not the total answer, however. To reduce the stability of the A-4 relative to the sc we must look elsewhere, possibly to the inclusion of nonlocality and more sophisticated handling of exchange and correlation.

The problem with the A-4 structure is actually part of a larger problem. For these large- Z ele-

ments, the second-order pseudopotential theory is most successful when small distortions from a given structure are considered. As noted by AOM, it seems usually less successful when the cohesive energies of rather disparate structures are considered.

Despite the problems, the fact that the orthorhombic-A-7 relative energies show the correct trends and the fact that the first order A-7-sc transition comes out of the calculations suggest strongly that we are beginning to understand the structural behavior of black P from a microscopic point of view.

ACKNOWLEDGMENTS

I have benefitted from stimulating and helpful conversations with Professor H. Bilz, Professor M. Cardona, Professor M. H. Cohen, Professor L. M. Falicov, Professor H. Fritzsche, Professor J. C. Jamieson, Professor W. A. Harrison, Professor V. Heine, Professor M. J. G. Lee, and Professor D. Weaire, Dr. J. Hafner, Dr. W. B. Holzapfel, and S. Schiferl. Dr. J. Hafner also provided the computer program for calculating the Ewald constants with the Ewald-Fuchs method and made many useful suggestions to improve the manuscript. The help of the staffs of the computation centers at the University of Chicago and at the Max-Planck-Institut für Festkörperforschung, Stuttgart is also gratefully acknowledged. This work was supported in part by NSF No. DES 73-00636 A02 and also benefitted from support of the Materials Science Research Laboratory by the NSF and from the U.S. Dept. of Energy. I am also very grateful for a NATO fellowship to support my stay at the Max-Planck-Institut.

*Present address: Los Alamos Scientific Lab., Los Alamos, N. M. 87545.

¹R. W. G. Wyckoff, *Crystal Structures* (Wiley, New York, 1963), Vol. I.

²J. Donohue, *The Structures of the Elements* (Wiley, New York, 1974).

³J. C. Jamieson, *Science* **139**, 1291 (1963).

⁴E. Parthé, *Z. Kristallogr. Kristallphys. Kristallchem.* **115**, 52 (1961).

⁵V. Heine and D. Weaire, *Solid State Phys.* **24**, 249 (1970) and references therein.

⁶W. A. Harrison, *Pseudopotentials in the Theory of Metals* (Benjamin, New York, 1966).

⁷J. Hafner, *Phys. Status Solidi B* **56**, 579 (1973); **57**, 101 (1973); **57**, 497 (1973).

⁸T. Schneider and E. Stoll, *Solid State Commun.* **8**, 1729 (1970).

⁹R. Pynn and I. Ebbsjö, *J. Phys. F* **1**, 744 (1971).

¹⁰J. Moriarty, *Phys. Rev. B* **8**, 1339 (1973).

¹¹J. Hafner and H. Eschrig, *Phys. Status Solidi B* **72**,

179 (1975).

¹²J. Hafner, *Z. Phys. B* **22**, 351 (1975); **24**, 41 (1976).

¹³V. Heine and D. Weaire, *Phys. Rev.* **152**, 603 (1966).

¹⁴J. E. Inglesfield, *J. Phys. C* **1**, 1337 (1968); **4**, 1003 (1971).

¹⁵D. Weaire, *Phys. Status Solidi* **42**, 767 (1970).

¹⁶D. Weaire and A. R. Williams in *The Physics of Semimetals and Narrow Gap Semiconductors*, edited by Carter and Bate (Pergamon, Oxford, 1971).

¹⁷Y. Abe, I. Okoshi, and A. Morita, *J. Phys. Soc. Jpn.* **42**, 504 (1977).

¹⁸J. Hafner, *Phys. Rev. B* **10**, 4151 (1974).

¹⁹M. H. Cohen, L. M. Falicov, and S. Golin, *IBM J. Res. Dev.* **8**, 215 (1964).

²⁰V. Heine and R. O. Jones, *J. Phys. C* **2**, 719 (1969).

²¹A description of the Strukturbericht notation for the elements is given in the appendix of C. S. Barrett and T. B. Massalski, *Structure of Metals* (McGraw-Hill, New York, 1967).

²²B. Morosin and J. E. Schirber, *Solid State Commun.*

- 10, 249 (1972).
- ²³J. Kasper, in *Transactions of the American Crystallographic Association: Proceedings of the Symposium on "Crystal Structures at High Pressures,"* edited by D. B. McWhan (American Crystallographic Association, New York, 1969).
- ²⁴B. Morosin and J. E. Schirber, *Phys. Lett. A* **30**, 512 (1969).
- ²⁵D. Schiferl, *J. Appl. Phys.* **48**, 24 (1977).
- ²⁶T. N. Kolobyanina, S. S. Kabalkina, L. F. Vereshchagin, and L. V. Fedina, *Zh. Eksp. Teor. Fiz.* **55**, 164 (1968) [*Sov. Phys.-JETP* **28**, 88 (1969)].
- ²⁷L. F. Vereshagin and S. S. Kabalkina, *Zh. Eksp. Teor. Fiz.* **47**, 414 (1964) [*Sov. Phys.-JETP* **20**, 274 (1965)].
- ²⁸S. S. Kabalkina, L. F. Vereshchagin, and V. P. Mylou, *Dokl. Akad. Nauk. SSSR* **152**, 585 (1963) [*Sov. Phys.-Dokl.* **8**, 917 (1964)].
- ²⁹D. B. McWhan, *Science* **176**, 751 (1972).
- ³⁰T. R. R. McDonald, E. Gregory, G. S. Barberich, D. B. McWhan, T. H. Geballe, and G. W. Hull, *Phys. Lett.* **14**, 16 (1965).
- ³¹R. M. Brugger, R. B. Bennion, and T. G. Worlton, *Phys. Lett. A* **24**, 714 (1967).
- ³²M. L. Cohen and V. Heine, *Solid State Phys.* **24**, 37 (1970).
- ³³R. W. Shaw, Jr., *J. Phys. C* **2**, 2335 (1969).
- ³⁴M. Appapillai and A. R. Williams, *J. Phys. F* **3**, 759 (1973).
- ³⁵J. F. Janak, *Solid State Commun.* **20**, 151 (1976).
- ³⁶Atomic units (a.u.) are used throughout unless otherwise noted. These are the units when $h=m=e=1$.
- Energies are in hartrees (1 hartree=1 a.u.=27.21 eV).
- ³⁷C. A. Sholl, *Proc. Phys. Soc.* **92**, 434 (1967).
- ³⁸K. Fuchs, *Proc. R. Soc. A* **151**, 585 (1935).
- ³⁹J. Hafner (private communication).
- ⁴⁰J. Hubbard, *Proc. R. Soc. A* **243**, 336 (1958).
- ⁴¹L. J. Sham, *Proc. R. Soc. A* **283**, 33 (1965).
- ⁴²P. J. Lin and L. M. Falicov, *Phys. Rev.* **142**, 441 (1966).
- ⁴³L. M. Falicov and P. J. Lin, *Phys. Rev.* **141**, 562 (1966).
- ⁴⁴N. W. Ashcroft, *Phys. Lett.* **23**, 48 (1966).
- ⁴⁵D. Schiferl and C. S. Barrett, *J. Appl. Crystallogr.* **2**, 30 (1969).
- ⁴⁶C. S. Barrett, P. Cucka, and K. Haefner, *Acta Crystallogr.* **16**, 451 (1963).
- ⁴⁷P. Cucka and C. S. Barrett, *Acta Crystallogr.* **15**, 865 (1962).
- ⁴⁸M. Born and K. Huang, *Dynamical Theory of Crystal Lattices* (Oxford University, London, 1954).
- ⁴⁹D. R. Penn, *Phys. Rev.* **128**, 2093 (1962).
- ⁵⁰G. Srinivasan, *Phys. Rev.* **178**, 1244 (1969).
- ⁵¹J. A. Van Vechten, *Phys. Rev.* **170**, 773 (1968).
- ⁵²V. Heine (private communication).
- ⁵³Y. Onodera, *Solid State Commun.* **11**, 1397 (1972).
- ⁵⁴D. Schiferl, *Phys. Rev. B* **10**, 3316 (1974).
- ⁵⁵D. D. Wagman *et al.*, *Selected Values of Chemical Thermodynamic Properties*, National Bureau of Standards Technical Note No. 270 (U.S. GPO, Washington, D. C., 1968).